Discreteness effects in a reacting system of particles with finite interaction radius

S. Berti,[1] C. López,[2] D. Vergni,[3] and A. Vulpiani[4,5]
[1]*Department of Mathematics and Statistics, University of Helsinki, P. O. Box 68, FIN-00014 Helsinki, Finland*
[2]*Instituto de Física Interdisciplinar y Sistemas Complejos IFISC (CSIC-UIB), Campus de la Universitat de les Illes Balears, E-07122 Palma de Mallorca, Spain*
[3]*Istituto Applicazioni del Calcolo (IAC)-CNR, Viale del Policlinico, 137, I-00161 Roma, Italy*
[4]*Dipartimento di Fisica and INFN, Università di Roma "La Sapienza," P.zle Aldo Moro 2, I-00185 Rome, Italy*
[5]*INFM-SMC, Piazzale Aldo Moro 2, I-00185 Rome, Italy*
(Received 10 April 2007; revised manuscript received 13 September 2007; published 28 September 2007)

An autocatalytic reacting system with particles interacting at a finite distance is studied. We investigate the effects of the discrete-particle character of the model on properties like reaction rate, quenching phenomenon, and front propagation, focusing on differences with respect to the continuous case. We introduce a renormalized reaction rate depending both on the interaction radius and the particle density, and we relate it to macroscopic observables (e.g., front speed and front thickness) of the system.

DOI: 10.1103/PhysRevE.76.031139 PACS number(s): 05.40.−a, 82.39.−k, 82.40.−g

I. INTRODUCTION

Most of the chemical and biological processes that appear in nature involve the dynamics of particles (e.g., molecules or organisms) that diffuse and interact with each other and/or with external forces [1–3]. If the total number of particles per unit volume, N, is very large, a macroscopic description of the system in terms of continuous fields, e.g., density or concentration, is usually appropriate. A prototypical model for these reaction-diffusion systems is the Fisher-Kolmogorov-Petrovskii-Piskunov (FKPP) equation [4,5] describing the spatiotemporal evolution of a concentration

$$\partial_t \theta(x,t) = D\partial_{xx}^2 \theta + p\theta(1-\theta), \tag{1}$$

where D is the diffusion coefficient, p is the reaction rate that determines the characteristic reaction time, $\tau=1/p$, and $\theta(x,t)$ is the concentration field (for simplicity we have assumed one spatial dimension). It is well-known [1,6,7] that Eq. (1) admits uniformly translating solutions—fronts—with a speed $v_0=2\sqrt{Dp}$ and a front thickness $\lambda_0=8\sqrt{D/p}$. Formally, one can have fronts with any speed; however, in [4] it has been proven that only speeds $v \geqslant v_0$ are possible. In addition (see [6,8]) there exists a selection mechanism such that $v=v_0$ is the unique possibility, at least with nonpathological initial conditions. The above results do not depend on the precise details of the reaction rule. Replacing in Eq. (1) $\theta(1-\theta)$ with a convex function $g(\theta)$, with $g(\theta)>0$ for $0<\theta<1$, $g(0)=g(1)=0$, and $g'(0)=1$, $g'(1)<0$, one has the same behavior for v_0 and λ_0 [8].

On the other hand, if the number of particles per unit volume is not very large, the continuous description might be inappropriate. In such a case, one can consider a discrete particle model with N particles whose positions $\mathbf{x}_\alpha(t)$ evolve according to the Brownian motion

$$\frac{d\mathbf{x}_\alpha(t)}{dt} = \sqrt{2D}\boldsymbol{\eta}_\alpha, \quad \alpha = 1, \ldots, N, \tag{2}$$

where $\boldsymbol{\eta}_\alpha$ are white noise terms. Moreover, each particle is characterized by a *color* $C_\alpha(t)$ which determines the particle type. The model is completed by the reaction *rule* between particles. In order to obtain an autocatalytic reaction

$$A + B \xrightarrow{p} 2B, \tag{3}$$

one can consider just two types of particles $C=0$ (unstable) and $C=1$ (stable) that correspond to the species A and B, respectively, with the following dynamics: particles of type 1 always remain 1, and particle 0 changes to 1 with a given probability that depends both on p, the reaction rate, and on how many 1 particles are around it. It is not difficult to realize that in a suitable continuum limit, Eq. (1) gives the evolution of the *color concentration* of this microscopic system (see Sec. II). The aim of this work is precisely to study the case in which the density of individuals is small, and therefore the discrete nature of the system can play a role [9,10].

Several approaches have been adopted to investigate the relevance of the correction to the continuum limit. On one side, it has been assumed that the dynamics of the system is given by deterministic macroscopic equations, like Eq. (1), with an additional noise term of order $1/\sqrt{N}$ accounting for microscopic fluctuations originated by the finite number of particles [11]. On the other side, following the work of Brunet and Derrida [12], this problem has been successfully studied by using a cutoff at the density value $1/N$ for the continuous field equations. This has been employed to determine corrections to some front properties in FKPP-like equations (see [13] for a review). In particular, it has been shown that the deviation from the continuous value of the front speed is of the order $1/(\ln N)^2$, which is rather significant [12].

More recently, Kaneko and co-workers [14] analyzed the dynamics of some chemical reactions, studying the influence of the molecular discreteness. They identify typical length scales in the system which may allow one to discriminate between the *continuous* behavior and the *discreteness-influenced* one. They report transitions to a novel state with symmetry breaking that is induced by discreteness, but they do not investigate features of front propagation. A crucial quantity is the so-called Kuramoto length, $l_K=\sqrt{2D\tau}$, which

measures the typical distance over which an unstable particle diffuses during its lifetime (note that $\tau=1/p$ can be interpreted as the average lifetime, i.e., the time particles live before they react). When the typical interparticle distance is much smaller than l_K, concentration can be regarded as continuous. On the other hand, when there are not many particles within a region of size l_K, discreteness effects should be taken into account [14].

In our work we study the interplay between length scales in the problem, our principal aim being to explain the effects of the discrete nature of the system on properties such as reaction rate, quenching, and front speed. Differently from most of the works in discrete reaction-diffusion systems, we do not consider a lattice model. Particles diffusively move in space and interact when their distance is smaller than an interaction radius R, which corresponds to a natural length scale appearing in many chemical and biological systems [10,15]. We study several properties of the system as a function of R, realizing, via comparison of different length scales, when the effects of discreteness have a dominant role. As expected, the continuum limit is described by the FKPP equation. Nevertheless we remark that in order to have the proper continuum limit it is not sufficient to have a very large density of particles. The discrete model results are found to differ from those valid in a continuous description both at a quantitative level, small changes in the behavior of some observables, and at a qualitative one, that is, the system evolution drastically changes. We discuss the problem in the framework of chemical reactions but everything can be translated to the context of population dynamics.

The paper is organized as follows. In the next section we introduce the particle model for the autocatalytic reaction. In Sec. III we study the renormalized reaction rate of the system when particles of both types are in a closed vessel, initially uniformly distributed at random in space. In Sec. IV we study quenching phenomena when B particles can turn into A particles; this causes the emergence of new properties that will be studied in detail. Then, in Sec. V we investigate the front properties of the model by choosing a proper initial condition and considering an infinite system in the propagation direction. Section VI summarizes our conclusions.

II. MODEL

Consider N particles in a two-dimensional box of size $L_x \times L_y$. Each particle is identified by its position, $\mathbf{x}_\alpha(t)$, and its *color*, $C_\alpha(t)$, indicating the particle type. To specify the dynamics it is necessary to give the evolution rule for the position and the interaction rule between particles (chemistry). Space will be considered continuous while time will be discrete (with time step Δt). Particle dynamics is synchronous, i.e., all particle properties are updated at the same time.

The position evolution is given by

$$\mathbf{x}_\alpha(t+\Delta t) = \mathbf{x}_\alpha(t) + \sqrt{2D\Delta t}\,\mathbf{u}_\alpha(t), \quad \alpha = 1, \ldots, N, \tag{4}$$

where D is the diffusion coefficient, $\mathbf{u}_\alpha(t)=[u_{\alpha,1}(t), u_{\alpha,2}(t)]$ are stochastic Gaussian variables with the properties $\langle \mathbf{u}_\alpha(t)\rangle = 0$ and $\langle u_{\alpha,i}(n\Delta t) u_{\beta,j}(m\Delta t)\rangle = \delta_{ij}\delta_{\alpha\beta}\delta_{mn}$, i.e., particles perform a discrete-time Brownian motion.

Let us start with the homogeneous case (premixed initial conditions). As already mentioned, to model an autocatalytic reaction (3), we consider two kinds of particles: type A particles, $C_\alpha=0$ (unstable), and type B particles, $C_\alpha=1$ (stable). Their chemical evolution is given by the following stochastic process:

(1) if $C_\alpha(t)=0$ then $C_\alpha(t+\Delta t)=1$ with probability $P_{AB} = W_{AB}\Delta t$; and

(2) if $C_\alpha(t)=1$ then $C_\alpha(t+\Delta t)=1$.

The probability (per unit time) W_{AB} depends on the number of stable particles within the interaction radius. In fact, when particles, of any type, are homogeneously distributed in space, the autocatalytic reaction (3) is expected to obey the mass action law $\frac{d\Theta_A}{dt} = -p\Theta_A\Theta_B$, where Θ_A and Θ_B are the (spatially uniform) concentrations of particles A and B, respectively, with $\Theta_A+\Theta_B=1$. The probability that a particle A (labeled with the index k) changes into a B particle is assumed to be

$$W_{AB}^k = p\frac{N_B^k(R,t)}{\langle N_{loc}(R)\rangle} = p\frac{N_B^k(R,t)}{\pi R^2\rho}, \tag{5}$$

where $N_B^k(R)$ indicates the number of B particles within the interaction radius R around the kth particle A, $\langle N_{loc}(R)\rangle$ is the spatial average number of particles (of any type) in a radius R, and $\rho=N/(L_xL_y)$ is the density of particles.

In a suitable limit the previous probabilistic rule converges to a reaction equation, i.e., a homogeneous FKPP equation, as discussed in the following. Let $N_A(t)$ and $N_B(t)$ be the total number of A and B particles, respectively; of course $N=N_A(t)+N_B(t)$ is constant. The dynamics of the number of B particles is given by the discrete stochastic process

$$N_B(t+\Delta t) = N_B(t) + \sum_{k=1}^{N_A(t)} y_k, \tag{6}$$

where k is the index identifying A particles and y_k is a discrete random variable which is 1 with probability $\Delta t W_{AB}^k$ (when the kth particle A changes into a B particle), and is 0 with probability $1-\Delta t W_{AB}^k$ (when the kth particle A does not change). For the expected value of $N_B(t)$ one has, in a mean field approximation, which is expected to hold in the homogeneous case and when the number of particles, N, is very large,

$$E[N_B(t+\Delta t)] = E[N_B(t)] + \frac{p}{\pi R^2\rho}E\left(\sum_{k=1}^{N_A} N_B^k(R,t)\right)\Delta t. \tag{7}$$

The quantity $E[N_B^k(R,t)]$ does not depend on k. Therefore

$$\begin{aligned} E[N_B(t+\Delta t)] &= E[N_B(t)] + pE[N_A(t)]\frac{E[N_B(R,t)]}{\pi R^2\rho}\Delta t \\ &= E[N_B(t)] + p\{N - E[N_B(t)]\}\frac{E[N_B(R,t)]}{\pi R^2\rho}\Delta t. \end{aligned} \tag{8}$$

After a little algebra we obtain

$$\frac{d}{dt}\Theta_B(t) = \lim_{\Delta t \to 0} \frac{\Theta_B(t+\Delta t) - \Theta_B(t)}{\Delta t}$$

$$= p[1 - \Theta_B(t)]\frac{E[N_B(R,t)]}{\pi R^2 \rho}, \tag{9}$$

where $\Theta_B = E[N_B(t)]/N$ indicates the expected average concentration of B particles. In the case of an infinite number of spatially premixed particles the last term on the right-hand side of the above relation becomes $\Theta_B(t)$ and we finally obtain the reaction equation

$$\frac{d}{dt}\Theta_B(t) = p[1 - \Theta_B(t)]\Theta_B(t). \tag{10}$$

For very small density, and/or in the nonhomogeneous case, Eq. (8) fails and the system cannot be described by simple reaction equations such as Eqs. (9) and (10) (see also next section and, in particular, Fig. 5).

Concerning the relevant length scales of the system one can identify the following ones: (i) the mean nearest-neighbor distance between particles (in the homogeneous case) $d_m = \frac{1}{2\sqrt{\rho}} = \sqrt{\frac{L_x L_y}{4N}}$; (ii) the interaction radius, R; (iii) the Kuramoto length scale, l_K; and (iv) the size of the system L. It is expected that the continuum limit is obtained when $d_m \ll R \ll l_K \ll L$. While the scale separation between d_m and L can be easily achieved, in many situations it might happen that the condition $R \ll l_K$ is not verified, or that R is of the same order of d_m. In this case the evolution of the system could be very different from that of the continuum FKPP limit. It is the objective of this work to investigate some properties of the model in this regime.

Before starting with the discussion of the numerical results, some comments follow about the role of diffusion. Since we introduce the natural length scale of the interaction, R, a diffusive time related to this distance arises, $t_D(R) = R^2/D$. When this time is much smaller than the reaction time $\tau = 1/p$ the system is locally homogenized before reaction happens. In order to focus on the reaction properties rather than on the diffusive effects we work in the limit $t_D \gg 1/p$.

III. PREMIXED PARTICLES IN CLOSED BASINS

First we study the model in a closed vessel, where, as the initial condition, particles of both types are premixed and uniformly randomly distributed in space. In such a case, the system evolution necessarily ends with the complete filling of the box with type B particles. Therefore the most significant physical quantity is the filling rate of B particles, which is related to the reaction rate. We proceed by fixing the value of R and varying N in order to explore different situations: (a) continuum limit, $d_m \ll R$ and (b) the effect of discreteness, $d_m \gtrsim R$. In this case, at variance with front propagation properties discussed in Sec. V, we will see that the Kuramoto length does not play a fundamental role. The basic reason for this is the spatially random distribution of particles.

We adopt periodic boundary conditions on a square domain of side $L_x = L_y = 1$; the reaction rate is set to $p = 1$; and averages are numerically computed over a large number of noise realizations.

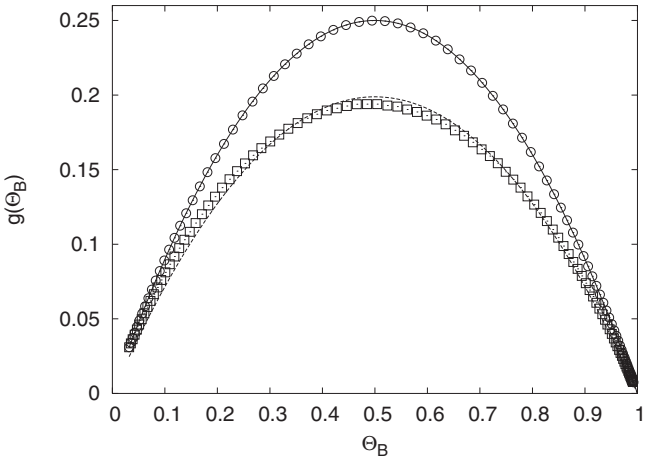

FIG. 1. The growth rate $g(\Theta_B)$ vs Θ_B [see Eq. (11)] for $N = 1000$ (□), and $N = 100\,000$ (○) with $p = 1$, $D = 0.001$, and $R = 0.05$; the initial concentration corresponds to 97% of type A particles and 3% of B particles, uniformly distributed. The solid and the dashed lines correspond to the quantity $p_R(N)\Theta_B(1-\Theta_B)$, where $p_R(N)$ is fitted from numerical results of the discrete particle model: the solid line is for $p_R(N) = 1$ and the dashed line for $p_R(N) = 0.8$.

Since particles are well-premixed, the process is spatially homogeneous, and we may assume that the growth rate of $\Theta_B(t)$ is [see Eq. (9)]

$$g(\Theta_B) = p[1 - \Theta_B(t)]\frac{E[N_B(R,t)]}{\pi R^2 \rho}. \tag{11}$$

In the case of large particle density one expects that $g(\Theta_B) = p\Theta_B(1-\Theta_B)$, therefore it is natural to assume that for finite N one can replace Eq. (11) with

$$g(\Theta_B) = p_R(N)\Theta_B(1 - \Theta_B), \tag{12}$$

where $p_R(N)$ is a renormalized reaction rate of the discrete particle model. In this way the evolution of Θ_B is given by a reaction equation with a *renormalized* (R-and N-dependent) reaction probability, where $\tau_R(N) = 1/p_R(N)$ is the renormalized reaction time for the system. Note that $p_R(N)$ contains all of the dependence of our system on the interaction radius and the number of particles. This is, therefore, the proper quantity to consider in order to investigate the relevance of discreteness in the model.

In Figure 1 it is shown, for a given R, the function $g(\Theta_B)$, given by Eq. (12) for two different values of N. With the appropriate $p_R(N)$ value, the fit is rather good and, for large N, $p_R(N) \to p$.

The equation $\frac{d\Theta_B}{dt} = p_R(N)\Theta_B(1-\Theta_B)$ can be easily solved:

$$\Theta_B(t) = \frac{\Theta_B(0)e^{p_R(N)t}}{1 + \Theta_B(0)(e^{p_R(N)t} - 1)}. \tag{13}$$

Thus looking at the evolution of $\Theta_B = E[N_B(t)]/N$ and using Eq. (13) we have a value of $p_R(N)$ which is, in principle, different from the one in Eq. (12). In Fig. 2, we show Θ_B

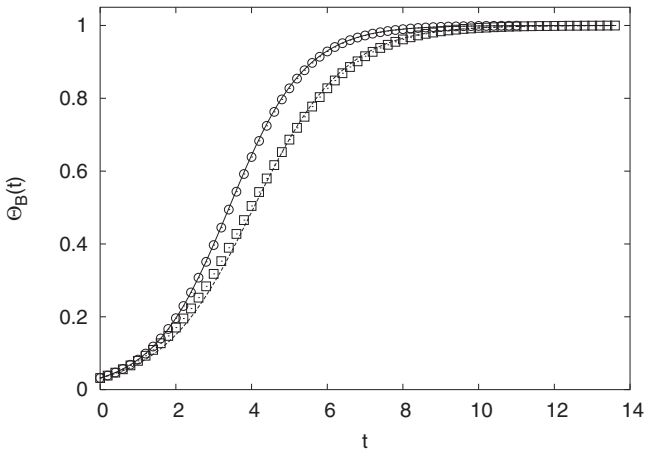

FIG. 2. $\Theta_B(t)$ versus t in the same experimental asset (and using the same symbol) of Fig. 1. The solid and the dashed lines correspond to the fit of Eq. (13) to the experimental measures. In particular the solid line is for $p_R(N)=1.0$ and the dashed line for $p_R(N)=0.82$.

versus time, as obtained from the numerical simulation of the particle model, and the best fit using Eq. (13) from which a value of $p_R(N)$ comes out. Let us observe that there are other different procedures to define a *renormalized reaction probability* for a particle system. They all have an empirical character but it suffices that they indicate quantitative differences in the reaction activities. In the present case, the rates obtained using Eq. (12) or Eq. (13) are very similar, and from now on we use only the last one. As previously shown in Fig. 1, for large N the value of $p_R(N)$ goes to the continuum limit p. In Fig. 3, the renormalized reaction probability versus N (at fixed R) is plotted. It can be seen that the continuum limit, $p_R(N)=p$, is obtained with good accuracy for large N values, as expected.

More important for our purpose is the behavior of $p_R(N)$ versus R. With a fixed total number of particles, N, and a well premixed initial condition, we compute $p_R(N)$ varying

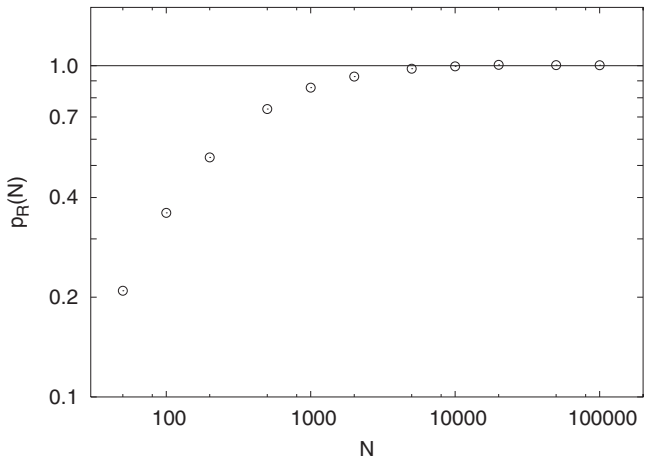

FIG. 3. $p_R(N)$ versus N. The parameters are the same as in Fig. 1. In particular, $R=0.05$, and the continuum limit is obtained for $N\approx 1000$ for which $d_m\approx 0.015$.

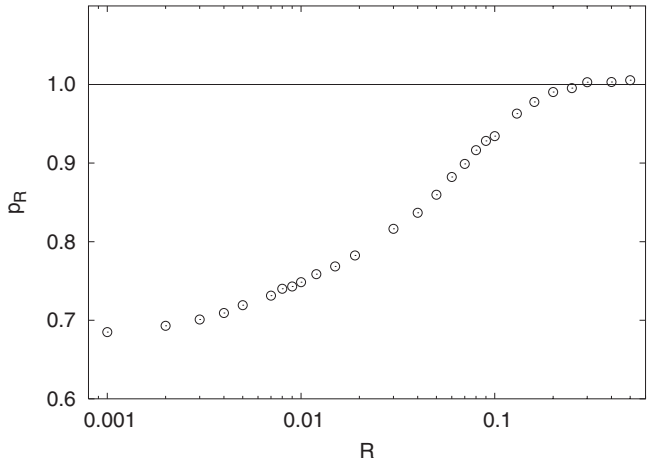

FIG. 4. The renormalized reaction probability $p_R(N)$ versus R, using the fit of Eq. (13). $N=1000$, $l_K=0.045$, and $d_m=0.0158$.

the interaction radius R (see Fig. 4). We observe that in the continuum limit ($d_m \ll R$) we recover $p_R(N)=p$. For small R, such that $d_m > R$, $p_R(N)$ seems to reach a constant value, which is around 30% smaller than the one of the reaction equation.

Few words have to be spent about the difference between the large N limit (Fig. 3) and the large R limit (Fig. 4). For the problem under discussion one has the same behavior of the continuum limit if $d_m \ll R$ irrespective of the value of the Kuramoto length. For example, in Fig. 4 one has $l_K \approx 0.045$ which is much smaller than the values of R for which the continuum limit holds. On the other hand, in the study of front properties we will see that the scenario is different and l_K can play a relevant role.

Now we want to discuss the dependence of the previous results on the chosen initial condition. We have already seen that the growth rate depends on the initial condition [see Eq. (9)]. In Fig. 5 we compare $g(\Theta)$ in the premixed case and when particles are initially separated in space. In this last

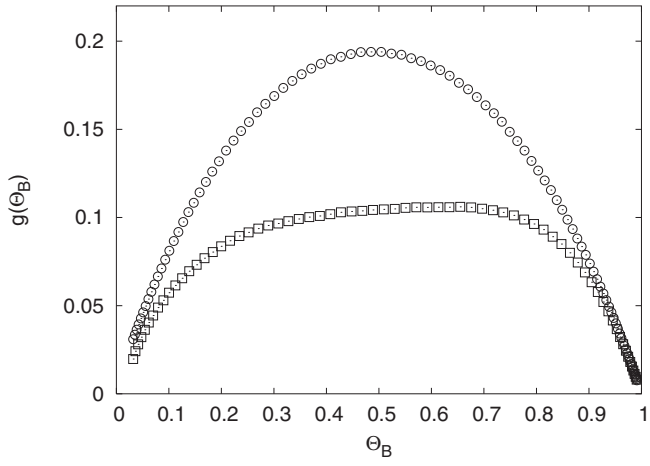

FIG. 5. $g(\Theta_B)$ vs Θ_B [see Eqs. (9) and (11)] for different initial conditions: (○) premixed and (□) B particles on the left of the system and A particles on the right. The parameters are $D=0.001$, $R=0.05$, $p=1$, and $N=1000$.

case it is rather evident that the approximations of Eqs. (11) and (12) cannot work very well.

Also in nonhomogeneous cases one may deduce an effective equation starting from Eq. (7) and using specific approximations (now considering, of course, the system geometry and the diffusion coefficient), however, this is beyond the aim of the present paper.

IV. POSSIBILITIES OF QUENCHING

Studies on the quenching phenomenon [16] show that in a continuous reaction-diffusion system advected by a velocity field front propagation may be suppressed, that is the reaction quenches, provided the initial size of the "hot" region is small enough. These results hold when the reaction kinetics is given by an ignition-type term such that $g(\Theta)=0$ for Θ smaller than a threshold value Θ_c. On the contrary, in a continuous FKPP system (1) quenching phenomena do not appear [17]. Here we show that in a *particle description* of an autocatalytic reactive system quenching can occur even if the continuous system does not quench.

Still considering premixed particles in a closed vessel, let us introduce the possibility that a stable particle (B) can turn into an unstable one (A). That is, beyond the autocatalytic reaction [3], we introduce a new reaction

$$B \xrightarrow{q} A, \tag{14}$$

where q is its rate. Therefore we have the following reaction rules:

(1) if $C_\alpha(t)=0$ then $C_\alpha(t+\Delta t)=1$ with probability $P_{AB}=W_{AB}\Delta t$, and

(2) if $C_\alpha(t)=1$ then $C_\alpha(t+\Delta t)=0$ with probability $Q_{BA}=W_{BA}\Delta t$.

W_{AB} is the same as the previous section, while $W_{BA}=q$ does not depend on the interaction radius R, since it is a single particle property.

The renormalized description of this model is given by

$$\frac{d\Theta_B(t)}{dt} = p_R(N)\Theta_B(1-\Theta_B) - q\Theta_B, \tag{15}$$

whose solution is

$$\Theta_B(t) = \Theta_{AS}\frac{\Theta_B(0)e^{\Lambda t}}{\Theta_{AS}+\Theta_B(0)(e^{\Lambda t}-1)}, \tag{16}$$

with $\Lambda=p_R(N)-q$ and $\Theta_{AS}=1-q/p_R(N)$. Two different scenarios now appear. If $p_R(N)<q$, for a given N, the reaction finishes. On the other side, when $p_R(N)>q$ we have a similar behavior as in the case with $q=0$. In Fig. 6 we show Θ_B vs t for different values of R. It is apparent that for large R the system behaves similarly to the case $q=0$ (including the continuum limit for the long time value of the concentration $1-q/p$). However, for R small enough the concentration asymptotically vanishes, that is we have a quenching phenomenon. In Fig. 7 we plot Λ vs R, obtained by fitting the analytical solution to the numerical results, as in the case of Fig. 4. For large R we approach the continuum limit and $\Lambda \to p-q$, while for small R we have quenching corresponding to negative values of Λ.

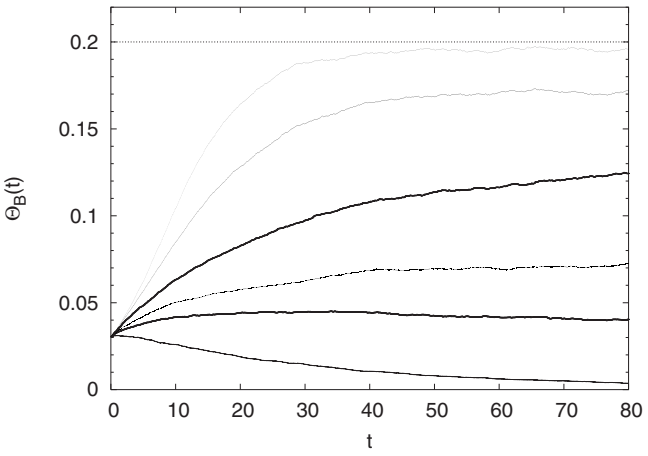

FIG. 6. Time evolution of $\Theta_B(t)$ for $R=0.5$, 0.1, 0.05, 0.03, 0.02, and 0.005 (from top to bottom), $N=1000$, and $D=0.001$; the straight line is the continuum limit asymptotic value $1-q/p$, with $p=1, q=0.8$. For $R<0.02$ the reaction quenches.

This is a relevant result, entirely due to the role of the interaction radius, R, which reflects the discrete character of the model in the quenching mechanism. Let us note that, at variance with the results in the previous section (which are just quantitative changes with respect to the continuous equation), now the discrete nature of the system is able to produce a feature (the quenching) which is absent in the continuum limit [17].

V. FRONT PROPERTIES

In the previous sections we have studied the dynamics of interacting particle systems in a closed container. We now focus on a different configuration, corresponding to well-separated chemicals in an open domain, and investigate evo-

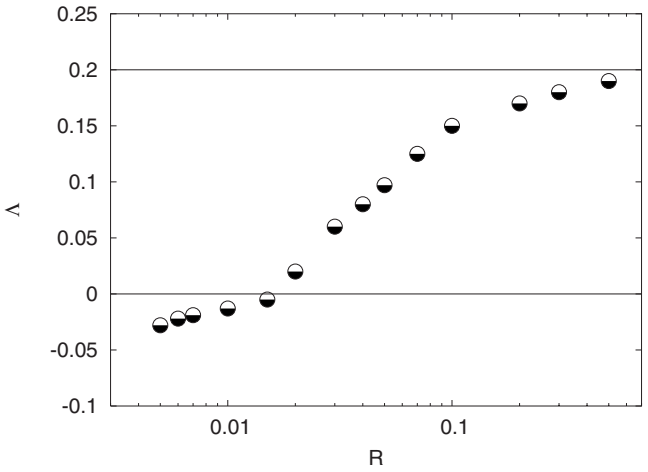

FIG. 7. Inverse characteristic time of the reacting process $\Lambda=p_R(N)-q$ as a function of the interaction radius R (with $p=1$, $q=0.8$); $N=1000$ and $D=0.001$. For large values of R, Λ tends to the continuum limit value $p-q$; for $R<0.02\Lambda$ becomes negative, highlighting the emergence of the quenching phenomenon.

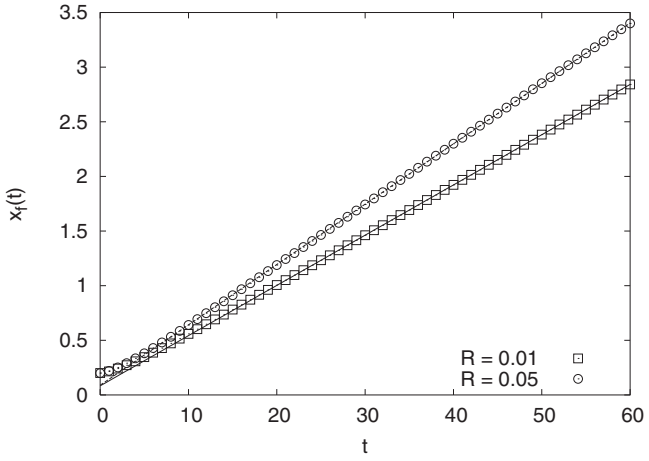

FIG. 8. x_f vs t. The system parameters are $L_x=5$, $L_y=1$, $D=0.001$, $p=1$, $N=5000$, and the initial number of B particles is 200. The slopes of the straight lines represent the front speed.

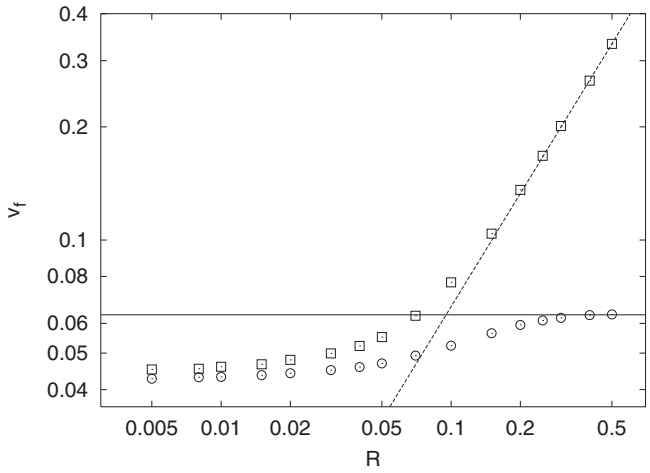

FIG. 9. (□) Front speed v_f versus R and (○) the prediction of formula (19), with $p_R(N)$ computed in closed domains with premixed particles. The parameters are the same as Fig. 8. The horizontal line is the value in the FKPP continuum limit (≈ 0.063), while the dashed line is the behavior $v_f \simeq R$. The Kuramoto length is $l_K=0.045$.

lution properties, such as front speed and thickness [18,19], in terms of the interaction radius.

In this section we take $L_y=1$, $L_x=5$, with periodic boundary conditions in the y direction, and rigid walls in the x direction. The burnt (type B) particles are initially concentrated in the leftmost part of the domain, so that a front propagating from left to right develops. The reaction term we use is just the autocatalytic one (3), i.e., $q=0$. We separately study the front speed and the front thickness.

A. Front speed

We can define the instant front position as

$$x_f(t) = L_x \frac{N_B(t)}{N}, \tag{17}$$

and compute the front speed by means of the simple relation

$$x_f(t) \simeq v_f t, \tag{18}$$

once the asymptotic behavior is reached. In Fig. 8 we show x_f versus time for different values of R. The speed v_f is obtained as the slope of the best fit to the curves in the region of linear growth of the front position.

We expect that, via the renormalized description of the FKPP equation, that is Eq. (1) with p replaced by $p_R(N)$, the front speed of the particle model at varying R should be

$$v_f = 2\sqrt{D p_R(N)}. \tag{19}$$

As shown in Fig. 5, different initial conditions for particles' distributions select different $p_R(N)$'s. Therefore, for an illustrative purpose, just to give a qualitative functional description of the simulation results, we use the $p_R(N)$ found in the case of mixed particles. The numerical results, reported in Fig. 9, show that at least for small R the front speed has a qualitative behavior similar to the FKPP case [Eq. (19)].

However, the significant discrepancy observed for large values of R cannot be explained by a simple difference in the initial particle distribution. This difference arises because the interaction radius becomes larger than the Kuramoto length

$$l_K = \sqrt{\frac{2D}{p}}, \tag{20}$$

and therefore the continuum FKPP limit does not hold. Indeed, in particle systems, when $R \geqslant l_K$ the interaction term establishes a connection between regions containing A particles and regions containing B particles that in the classical FKPP equation could not be connected. Therefore when $R \geqslant l_K$, it is not possible to obtain the continuum FKPP limit (1) even with an arbitrarily large number of particles. In Fig. 10 it is shown the front speed at varying R for various N. One can observe that at increasing N for small R the front speed approaches the FKPP value, while for large R the front speed does not depend on N and the value is definitely different from the FKPP value.

A simple argument explains the behavior of v_f for large R. The front speed is proportional to the front width times the reaction rate, e.g., in the FKPP equation $v_0 = 2\sqrt{Dp} \propto p\sqrt{D/p} \propto p l_K$. When the interaction radius is greater than the Kuramoto length it is reasonable to expect that the front width becomes proportional to R and so the front speed

$$v_f \propto p_R(N) R = \alpha R \quad \text{when } R \gg l_K, \tag{21}$$

in agreement with the results shown in Figs. 9–11 for various p. In particular, in the inset of Fig. 11 one can see the behavior of α as a function of p:

$$\alpha(p) = ap, \tag{22}$$

where a is a constant. This is not surprising because p is the continuum limit for the reaction rate which is reached asymptotically by the particle system, i.e., $p_R(N) \to p$ for large R.

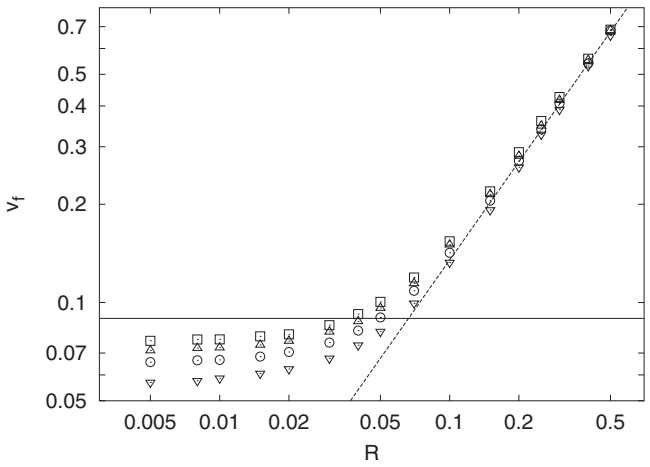

FIG. 10. The measured front speed v_f versus R for (▽) $N=5000$, (○) $N=10\,000$, (□) $N=20\,000$, and (△) $N=40\,000$. The horizontal line is the value in the FKPP continuum limit, while the dashed line is the behavior $v_f \simeq R$. In order to show a clear linear behavior for the asymptotic front speed here we use $p=2$, the Kuramoto length is $l_K=0.032$. The diffusion coefficient is $D=0.001$.

B. Front thickness

As a further confirmation of the previous results, we investigate the behavior of the front thickness at varying R. Note that in the continuum limit there are many ways to compute the front thickness of a propagating front [20]. In the particle case, however, it is not obvious how to define a front profile. We proceed by defining an averaged field that resembles the front shape. Essentially this is a histogram over particle positions. Fixing our attention on A particles, we define

$$\tilde{\Theta}_A(x,\Delta x;t) = \frac{N_A(x,\Delta x;t)}{N\Delta x}, \tag{23}$$

where $N_A(x,\Delta x;t)$ counts the number of A particles whose x coordinate lays between x and $x+\Delta x$. When the number of particles is large the value of Δx could be taken arbitrarily small whereas, in general, Δx has to be small, but at the same time large enough in order to avoid large fluctuations in $N_A(x,\Delta x;t)$. We use a relatively small Δx (few d_m) and we average $N_A(x,\Delta x;t)$ over many different realizations. The front shape of an FKPP system behaves as

$$\tilde{\Theta}_A(x,\Delta x;t) \sim \exp\{[x - x_f(t)]/l_A\}, \tag{24}$$

where l_A is the front thickness, and $x_f(t)$ the front position at time t. In Fig. 12 it is shown the exponential behavior of the front profile and the fit obtained from Eq. (24). In particular Eq. (24) works well in the central region of the front, i.e., where corrections due to the particle nature of the system are less important. Other measurements of the front profile provide similar results.

In Fig. 13 we plot the front thickness, l_A, computed for

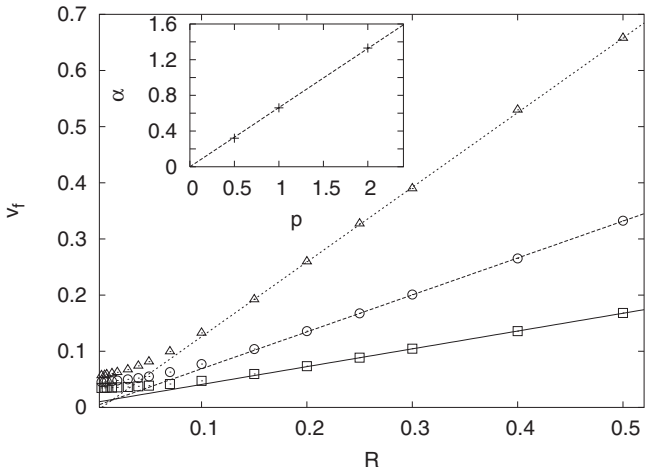

FIG. 11. Large R behavior of v_f in the cases $p=0.5$ (□), $p=1.0$ (○), and $p=2.0$ (△). In the inset the slope of the linear fit, α [see Eq. (22)], is shown as a function of p.

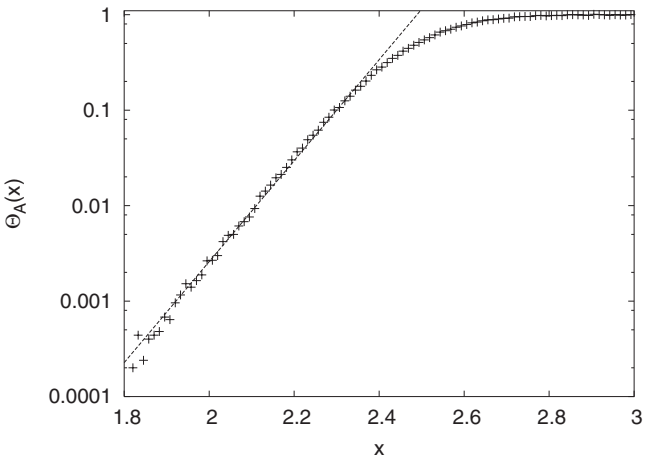

FIG. 12. The shape of the front $\tilde{\Theta}_A(x)$ (+) and the exponential fit of Eq. (24) (dashed line).

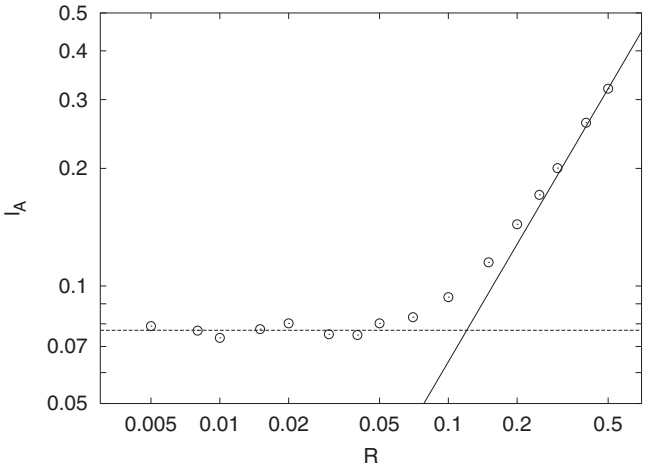

FIG. 13. Front thickness l_A versus R measured in the particle model (○). The dashed line corresponds to a constant value of the front speed (see Fig. 10), while the full line is the behavior $l_A \simeq R$. The value of the Kuramoto length is $l_K=0.045$.

different values of R. Again, for R smaller than the Kuramoto length the front thickness is constant, while for values of R greater than l_K the front thickness behaves as $l_A \propto R$. This result confirms the assumption of Eq. (21). The constant value reported in Fig. 13 (the dashed line) is only an indicative value to show that for $R < l_K$ the front thickness is constant, and it is not the FKPP value of the front width.

VI. SUMMARY AND CONCLUSIONS

In this work we studied the effects of the discrete-particle character in an autocatalytic reacting system. This was described in terms of chemical rules where two types of Brownian particles interact when they are at a distance smaller than a given radius R. We have shown that in a suitable continuum limit, and under well-defined conditions, the system is equivalent to a continuous reaction-diffusion model. The continuum limit holds, in general, when the average distance between particles is smaller than the interaction radius and the latter is smaller than the Kuramoto length. Moreover, we have focused on the differences that arise when the conditions for this limit are not fulfilled.

First we have studied the dynamics of the system for well-premixed initial conditions. In this case we have shown that only two length scales are relevant and the continuum limit arises when the mean distance among particles is much smaller than the interaction radius. Much of our analysis rests upon defining a renormalized reaction rate, $p_R(N)$, that depends on R and N and captures all the relevance of the discrete character of the model. We have analyzed the behavior of $p_R(N)$ with N and R. In particular, for large R the continuous description is valid ($p_R \to p$). On the contrary, for small R, p_R attains values smaller than p.

Then, still considering premixed initial conditions, we have studied the modified chemical dynamics $A+B \overset{p}{\to} 2B$, and $B \overset{q}{\to} A$. Even when p is larger than q, at variance with the continuous model, in the particle model one can have the possibility of quenching, which is obtained for small values of R. This is due to the particle nature of the model, since one can have that $p_R(N) < q$. This result for the particle model is a clear qualitative difference with respect to the continuous description.

Finally, in the context of front propagation, that is when particles are no longer initially well-premixed, a relevant result is that all three length scales are important for the system dynamics. We have shown that under particular conditions, increasing the particle density the system reaches a continuum limit which is definitely different from the continuum FKPP limit. For small R and a large number of particles the system has a qualitatively similar behavior of the FKPP model, i.e., the front velocity is proportional to $v_f = 2\sqrt{D p_R(N)}$. Nevertheless, for large R, $v_f \propto p_R(N) R$. The transition between these two regimes is given by the comparison between R and l_K (the Kuramoto length). When $R > l_K$ the FKPP behavior cannot be reached even for a very large number of particles. Similar results are obtained for the front thickness.

We conclude noting that many biological systems are characterized by the two main ingredients of our work: a finite distance for the interaction, and the exiguity of the number of organisms [2,21]. We hope that our work helps to clarify some shortcomings arising when a macroscopic description is attempted.

ACKNOWLEDGMENTS

We have benefited from a MEC-MIUR joint program (Italy-Spain Integral Actions). C.L. acknowledges support from FEDER and MEC (Spain) through Project CONOCE2 (FIS2004-00953). A.V. and D.V. acknowledge support from PRIN-MIUR grant "Dinamica Statistica di sistemi a molti e pochi gradi di libertà." We warmly acknowledge E. Hernández-García and S. Pigolotti for a critical reading of the manuscript.

[1] J. D. Murray, *Mathematical Biology* (Springer-Verlag, Berlin, 1993).
[2] G. Flierl, D. Grunbaum, S. Levin, and D. Olson, J. Theor. Biol. **196**, 397 (1999).
[3] T. Tél, A. de Moura, C. Grebogi and G. Károlyi, Phys. Rep. **413**, 91 (2005).
[4] A. N. Kolmogorov, I. Petrovskii and N. Piskunov, Bull. Univ. Moscow, Ser. Int. A **1**, 1 (1937).
[5] R. A. Fisher, Ann. Eugenics **7**, 355 (1937).
[6] W. van Saarloos, Phys. Rep. **386**, 29 (2003).
[7] J. Xin, SIAM Rev. **42**, 161 (2000).
[8] D. G. Aronson and H. F. Weinberger, Adv. Math. **30**, 33 (1978).
[9] W. R. Young, A. J. Roberts, and G. Stuhne, Nature (London) **412**, 328 (2001).
[10] E. Hernández-García and C. López, Phys. Rev. E **70**, 016216 (2004); C. López and E. Hernández-García, Physica D **199**, 223 (2004).
[11] C. R. Doering, C. Mueller, and P. Smereka, Physica A **325**, 243 (2003).
[12] E. Brunet and B. Derrida, Phys. Rev. E **56**, 2597 (1997).
[13] D. Panja, Phys. Rep. **393**, 87 (2004).
[14] Y. Togashi and K. Kaneko, Phys. Rev. Lett. **86**, 2459 (2001); Phys. Rev. E **70**, 020901(R) (2004).
[15] A. W. Visser and U. H. Thygesen, J. Plankton Res. **25**, 1157 (2003); C. López, Phys. Rev. E **72**, 061109 (2005).
[16] N. Vladimirova, P. Constantin, A. Kiselev, O. Ruchayskiy, and L. Ryzhik, Combust. Theory Modell. **7**, 487 (2003).
[17] J. M. Roquejoffre, Arch. Ration. Mech. Anal. **117**, 119 (1992); Ann. Inst. Henri Poincare, Anal. Non Lineaire **14**, 499 (1997).

[18] J. Mai, I. M. Sokolov, and A. Blumen, Europhys. Lett. **44**, 7 (1998); Phys. Rev. E **62**, 141 (2000).

[19] A. Lemarchand and B. Nowakovski, Europhys. Lett. **41**, 445 (1998).

[20] M. Abel, A. Celani, D. Vergni, and A. Vulpiani, Phys. Rev. E **64**, 046307 (2001).

[21] R. Durrett and S. A. Levin, Theor Popul. Biol. **46**, 363 (1994).